

A NOTE ON COPPER SUBSTITUTED NI-ZN FERRITE SYNTHESIZED BY SOL-GEL METHOD USING PEG

P. Prameela^{1*}, GSVRK Choudary², K S Rao³, K H Rao⁴

¹Department of Physics, Vel Tech, Avadi, Chennai, Tamil Nadu, India.

²Department of Physics, Bhavan's Vivekananda College of Science, Humanities and Commerce, Sainikpuri, Secunderabad, India.

³Department of physics, PBN College, Nidubrolu, India.

⁴RGU-IIIT Nuziveedu, Nuziveedu, Andhra Pradesh, India

ABSTRACT-The effect of copper substitution on initial permeability, Curie temperature, force constant and DC resistivity in Ni-Zn ferrite of composition $\text{Ni}_{0.65-x}\text{Cu}_x\text{Zn}_{0.35}\text{Fe}_2\text{O}_4$ has been presented. The variation in Curie temperature with copper concentration has been attributed to the changes in super exchange interaction between cations distributed over tetrahedral and octahedral sites of spinel lattice. The decrease in force constant, estimated from the absorption bands of FTIR spectra, with copper concentration suggests the lighter nature of the bonds. The observed high values of magnetic permeability, DC resistivity, and bulk density for the composition $x = 0.18$ suggest that copper substitution at lower concentrations yield useful electromagnetic properties in Ni-Zn ferrite system.

Keywords: FERRITES, PERMEABILITY, CURIE TEMPERATURE, DC RESISTIVITY, PEG.

1. Introduction:

Frequency dependence of magnetic permeability and its stability are important parameters for the effective use of ferrites in various applications. The frequency dispersion of magnetic permeability is an important feature at high frequencies to understand the domain wall mechanism and magnetic losses associated with the system [1]. Stability of magnetic permeability in a ferrite below 100 MHz depends on the domain wall behaviour, Curie temperature and DC resistivity [2]. Ni-Zn and Mn-Zn ferrites were subjected to extensive magnetic permeability studies by several research groups [3-5] because of their applications in several technological fields.

Among Ni-Zn ferrite systems, the composition $\text{Ni}_{0.65}\text{Zn}_{0.35}\text{Fe}_2\text{O}_4$ is one of the most versatile magnetic materials used in low and high frequency devices, due to its high resistivity, low dielectric losses, and good frequency stability of permeability. Interestingly, the processing of Ni-Zn ferrite nanoparticles in relation to unique magnetic properties was treated by several researchers by adopting various methods [6-7]. The sol-gel method was found to be reliable one in yielding fine particles [8] of the required size with high saturation magnetization, and low particle size. The method of preparation appears to be eco-friendly and has been adapted to a large scale and economic production by several researchers [9-11]. However, the information available in respect of the role of chelating agent in controlling the particle size, electric and magnetic properties is limited.

Recently, it was reported that the addition of copper to Ni-Zn ferrites could improve the magnetic properties as well as density [12]. A study on magnetic permeability with copper concentration up to $x = 0.30$ was reported in our earlier work [13] on nano crystalline $\text{Ni}_{0.65-x}\text{Cu}_x\text{Zn}_{0.35}\text{Fe}_2\text{O}_4$ ferrite. The Ni-Cu-Zn ferrites are soft magnetic materials, widely used to fabricate multilayer chip inductors and electromagnetic interference filters [14]. In continuation, the frequency dispersion of the magnetic permeability has been studied in the present investigation to elucidate the suitability of the material for high frequency applications.

2. Experimental Details

Nanoparticles of $\text{Ni}_{0.65-x}\text{Cu}_x\text{Zn}_{0.35}\text{Fe}_2\text{O}_4$, where x varies from 0.00 to 0.30 in steps of 0.06 were prepared by the sol-gel method using polyethylene glycol (PEG) as chelating agent. Analytical reagent grade, iron, nickel and zinc nitrates were used as ingredients in the required stoichiometric proportion. The weight ratio of the ferrite to the chelating agent was maintained at 1:3 and the details of the method of preparation of the samples were given elsewhere [14]. The dried (as-prepared) powder of each composition, annealed at 400 °C in air atmosphere for an hour before subjected to natural cooling was crushed thoroughly and pressed into pellets as well as toroids using polyvinyl alcohol as a binder. The pressed samples were further heat treated in air atmosphere for another hour at a temperature of 1050 °C to acquire higher magnetization and volume density.

2.1 Characterization

The formation of spinel structure of all the ferrite samples was confirmed in earlier publication [13] using X-ray Bruker advanced D8 X-ray diffractometer, in which the sample was irradiated by Cu-K α radiation ($\lambda = 1.5406 \text{ \AA}$). The room temperature infrared spectra of the samples were recorded using the FTIR spectrometer (Nicolet magna 550 model) in the range of 400-4000 cm^{-1} by KBr pellet method. The inductance measurement from 1 kHz to 13 MHz has been carried out on toroidal samples using a HP4192A LF Impedance analyser operated at very low voltage of 1 mV. Initial permeability is computed from the measured inductance using

$$\mu_i = \frac{L}{L_0}$$

where L_0 is the air core inductance, which is equal to $0.4606N^2h\log\left(\frac{OD}{ID}\right)$ micro henry [15] and N is the number of turns. The Curie temperature of the samples was measured using Soohoo method. The volume density measurement based on Archimedes' principle was compared with the X-ray density, estimated using the equation $d_x = 8M/Na^3$, where M is the molecular weight of the composition, N is the Avogadro's number and ' a ' is the lattice parameter. DC resistivity was measured by two-probe method with the help of digital nano ammeter model DNM-121. The average grain size of all the ferrite compositions was estimated from the SEM micrographs using linear intercept method, described in our previous paper [13].

3. Results and discussion

The volume density of $Ni_{0.65-x}Cu_xZn_{0.35}Fe_2O_4$ has been observed to decrease slightly with copper concentration up to $x = 0.12$ followed by a slow increase. The experimental and X-ray densities of the samples were shown in Table 1 along with the grain size values.

Table 1: Experimental, X-ray density, and average grain size for $Ni_{0.65-x}Cu_xZn_{0.35}Fe_2O_4$

Concentration (x)	Exptl. Density (g/cm ³)	X-ray density (g/cm ³)	Average grain size D (μm)
0.00	4.69	5.35	0.38
0.06	4.52	5.34	0.42
0.12	4.42	5.33	0.54
0.18	5.06	5.31	2.34
0.24	5.03	5.30	2.30
0.30	5.02	5.27	2.27

The variation in X-ray density has been observed to be meagre. The observed slight decrease in volume density for smaller initial concentrations of copper might be due to inter granular porosity developed at high annealing temperatures [16]. For concentration, above $x = 0.12$, substituted copper is expected to serve as a sintering agent [17] in promoting the grain growth by coalescing the grains and thereby reducing the pores in the ferrite material. The observed variation in experimental density appears to be in parallel to that of grain size, taken from the earlier report [13].

3.1 Fourier transform Infrared spectra

The room temperature FTIR spectra of all the copper substituted Ni-Zn ferrite samples are shown in figure 1. Each spectrum contains two significant absorption bands corresponding to tetrahedral and octahedral sites lying between 500-590 cm⁻¹ and 400-490 cm⁻¹. The observed bands around 590 cm⁻¹(ν_1) and 420 cm⁻¹(ν_2) have been attributed to the stretching vibrations of bonds between cation and oxygen ions at tetrahedral (A) and octahedral (B) sites respectively. Further, these bands are observed to shift towards the lower wave numbers with the copper concentration. The gradual increase in intensity of the octahedral band with copper concentration indicates that copper enters octahedral sites and replacing nickel ions. The variation in tetrahedral band intensity is too insignificant to throw any information related to copper occupancy at tetrahedral sites.

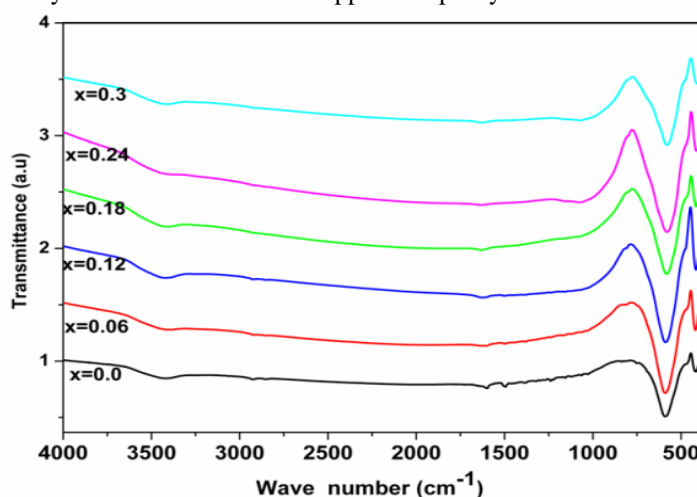


Figure 1: FTIR spectra of $Ni_{0.65-x}Cu_xZn_{0.35}Fe_2O_4$

The wave numbers of band positions corresponding to tetrahedral and octahedral metal complexes are presented along with force constant values in Table 2. In most of the Ni-Zn ferrite systems, nickel and zinc ions prefer to occupy octahedral and tetrahedral sites respectively, whereas, copper ions exist on both the sites, despite having a strong preference towards octahedral sites [18].

However, FTIR spectra of the investigation indicate that copper ions occupy octahedral sites only, replacing Ni^{2+} ions of comparatively smaller ionic radius and lower mass number.

Table 2: Tetrahedral and Octahedral peak wavenumbers, and force constant of octahedral site

Concentration (x)	Tetrahedral peak wave number (ν_1)	Octahedral peak wave number (ν_2)	Force constant K_o (10^5 dyne/cm)
0.00	590	417	1.59
0.06	590	418	1.60
0.12	588	417	1.59
0.18	582	417	1.59
0.24	581	415	1.57
0.30	579	409	1.53

The force constant for the octahedral site has been calculated from the equation [19] $K = 4\pi^2 c^2 \nu^2 \mu$, where c is the speed of light, ν is the wave number of band in cm^{-1} and μ is the reduced mass for Fe^{3+} and O^{2-} ions. The variation in the force constant of the octahedral site has been observed to be scanty up to copper concentration $x = 0.18$ followed by a decrease at higher concentration. In general, a lowering of the force constant for either site may be expected if the mean ionic charge for such a site is lowered. The lowered electrostatic energy would lead to a slight increase of the bond length and a reduction in the repulsive forces between the ions leading to a lower force constant. The increase in copper concentration displacing the nickel ions at octahedral sites and the formation of Cu^{+} ions could reduce the mean ionic charge of these sites and the process is responsible for the observed variation in band position and force constant. The site occupancy of copper and its state is further supported by considering the variation of DC resistivity with the increasing copper content.

Figure 2 shows the Curie temperature variation as a function of copper concentration. The observed decrease in Curie temperature is related to the site occupancy of copper ions and consequent changes in exchange interactions between ions over A and B sites.

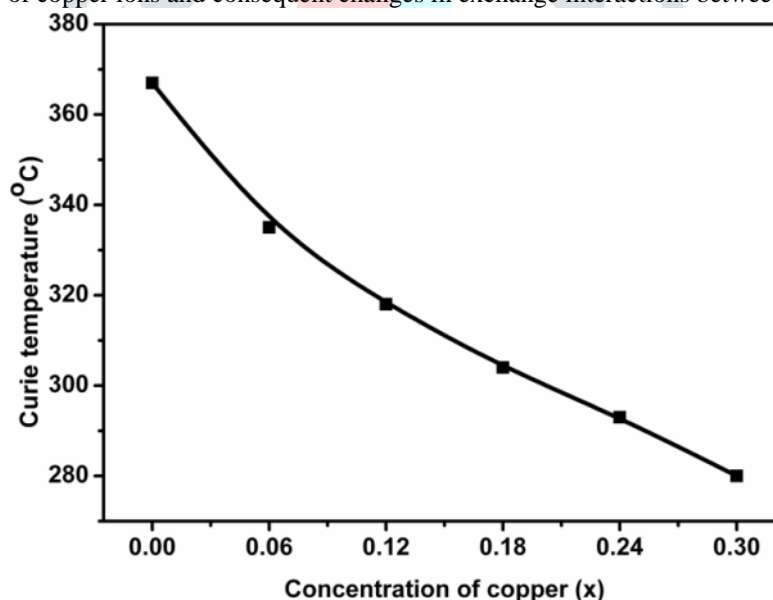


Figure 2: Variation of Curie temperature with concentration

The incorporation of diamagnetic copper replaces nickel at B-sites and reduces the magnetic moment of the B-sub lattice. The process weakens A-B exchange interaction which is reflected in the fall of Curie temperature with the increasing copper concentration. The fall of Curie temperature associated with the replacement of magnetic ions by diamagnetic ions has been a well-known phenomenon [19].

The variation in DC resistivity with increasing copper concentration in Ni-Zn ferrite system has been shown in figure 3. The resistivity is observed to increase with copper concentration up to $x = 0.18$ and then decreased at higher concentration.

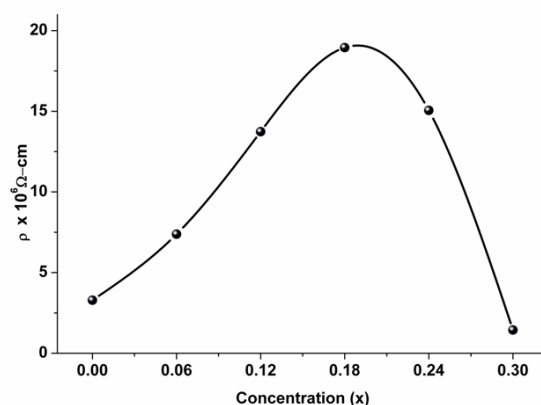


Figure 3: Variation of resistivity with copper concentration.

The DC resistivity of the basic nickel-zinc ferrite, $\text{Ni}_{0.65}\text{Zn}_{0.35}\text{Fe}_2\text{O}_4$ of the present investigation has been found to be higher than the reported in bulk samples of the same composition by other researchers [20]. The grain size is also lower than those of the bulk Ni-Zn ferrite of the same composition [21]. The higher DC resistivity and lower grain size clearly indicate that the sol-gel process is effective in providing smaller grains with more number of grain boundaries.

The observed dependence of DC resistivity with copper concentration can be explained basing on Verwey mechanism [19]. According to Verwey, the electronic conduction in ferrites is primarily due to hopping of electrons between the ions of the same element present in more than one valance state. In ferrite crystalline structure, the distance between two metal ions present at B-sites is smaller than the distance between a metal ion at B-site and another metal ion at A-site. The electron hopping between ions residing at B and A sites under normal conditions, therefore, has a very small probability as compared to that of hopping between ions at B-B sites. Hopping between ions at A-A sites will not take place for the simple reason that Fe^{2+} ions prefer to occupy B-sites only.

Higher annealing temperatures involved in the preparation of the samples may not rule out the presence of trace amounts of Fe^{2+} and Ni^{3+} ions in the product [22] and the hopping mechanism between Fe^{3+} - Fe^{2+} and Ni^{3+} - Ni^{2+} which contribute to the conduction process. As the incorporated copper replaces nickel present at octahedral site and reduces the carrier number due to the protection of $\text{Ni}^{2+} \rightarrow \text{Ni}^{3+}$ oxidation by copper content up to $x = 0.18$. Thus, hopping probability between ions of different valence states available at B-sites will be reduced and consequently the DC resistivity increases with the concentration of copper. At higher concentrations of copper, Cu^+ ions become significant and increasing hopping probability between Cu^+ and Cu^{2+} ions, thereby contributing to the gradual decrease in resistivity. Similar findings have been reported in respect of resistivity as a function of copper concentration in Ni-Zn bulk ferrite system [16].

3.2 Frequency dependence of initial permeability

Figure 4 shows the frequency dependence of initial permeability up to 13 MHz for copper substituted nickel zinc ferrite samples. The samples having higher copper concentration showed a distinct variation in permeability with frequency, whereas, the variations belonging to lower concentrations are overlapped. In general, initial permeability in nickel-zinc ferrites remains constant with frequency up to a certain value called critical frequency and then falls rapidly by a relaxation process at frequencies around a few megacycles per second. The initial permeability has been observed to be constant throughout the frequency range studied in all the samples except for $x=0.18$ and the critical frequency for this sample lies around 8 MHz. As the grain size and initial permeability are relatively less in other samples, the critical frequency has been expected to lie at frequencies beyond 13 MHz.

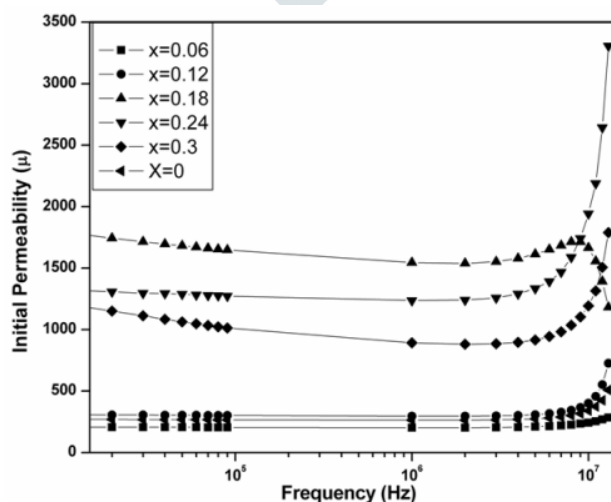


Figure 4: Frequency dispersion of permeability as a function of copper concentration

The Q factor is used as a measure of performance of the material for practical application. The Q factor is defined as $Q = 1/\tan\delta$, where, $\tan\delta$ gives the loss factor. Variation of magnetic loss tangents of the copper substituted nickel zinc ferrite samples with frequency is shown in figure 5. The quality factor of all the samples increases with increasing frequency, showing a peak, then decreases with frequency. The quality factor has been observed to decrease with increasing copper concentration, while the frequency corresponding to the peak has been observed to shift towards the higher frequency. The loss is due to lag of domain wall motion under alternating magnetic field, which is attributed to various domain defects [23], such as domain wall motion, domain wall bulging, localized variation of flux density etc., With the increase in domain size, losses increase at higher frequency (like eddy current losses) leading to decrease in Q-factor.

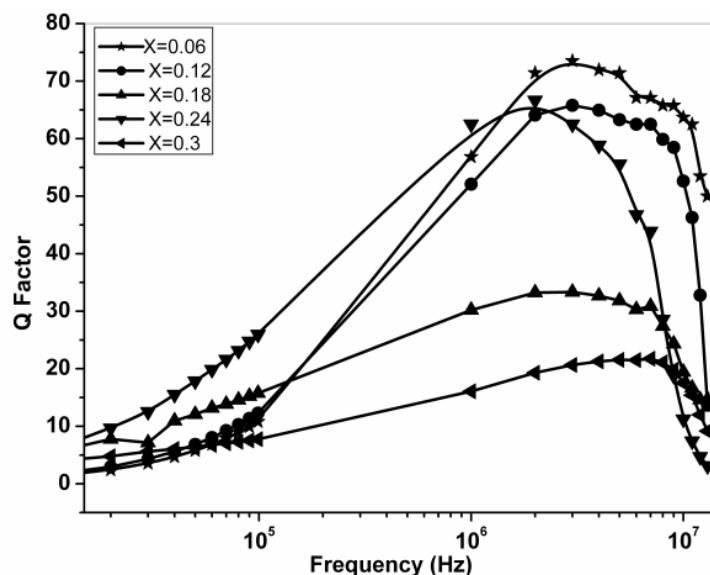


Figure 5: Variation of Q factor with frequency of copper substituted nickel zinc ferrites

3.3 Conclusion

The study establishes the occupancy of copper ions at octahedral sites. Remarkably, the initial permeability possessed by the composition having copper concentration $x = 0.18$ is a desirable value for MLCI applications.

Acknowledgements

The author is very much thankful to Physical Metallurgy Group, IGCAR for helping her in taking these measurements. My special thanks to M Siva Kumar from IIT Kanpur.

REFERENCE

1. A. S. Albuquerque, J. D. Ardisson, W. A. A. Macedo, M. C. M. Alves, J. Appl. Phys. 87, 4352 (2000)
2. Takanori Tsutaoka, Tatsuya Nakamura, Kenichi Hatakeyama, J. Appl. Phys. 82 (6), 3068 (1997)
3. Ulisandra Lima Ribeiro, Ricardo Silveira Nasar, Marinalva Cerqueira Nasar, and José Humberto de Araújo, Ceram. Int. 44(2018)723-727
4. Rastislav Dosoudil, Vladimír Olah and Vladimír Ďurman, Journal of ELECTRICAL ENGINEERING, 53(2002)143-148
5. Takanori Tsutaoka, JOURNAL OF APPLIED PHYSICS 93(2003)2789-2796
6. M. Rahimi, P. Kameli, M. Ranjbar, H. Hajhashemi and H. Salamati, J Mater Sci 48(2013) 2969-2976
7. Kh. Gheisari, Sh. Shahriari and S. Javadpour, J. Alloys. Compd 552(2013)146-151
8. K. Srinivasa Rao, S. V. Ranga Nayakulu, M. Chaitanya Varma, G. S. V. R. K. Choudary and K. H. Rao, J. Magn. Magn. Mater. 451 (2018) 602-608.
9. M. Sivakumar, S. Kanagesan, K. Chinnaraj, R. Suresh Babu and S. Nithiyantham, J. Inorg. Organomet. Polym. Mater. 23(2013) 439-445.
10. Shifeng Yan, Jianxin Geng, Li Yin and Enle Zhou, J. Magn. Magn. Mater. 277(2004) 84-89.
11. A. Mahesh Kumar, M. Chaitanya Varma, Charu Lata Dube, K. H. Rao and Subhash C. Kashyap, J. Magn. Magn. Mater. 320(2008) 1995-2000.
12. J. J. Shrotri, S. D. Kulkarni, C. E. Deshpande, A. Mitra, S. R. Sainkar, P. S. Anil Kumar and S. K. Date, Mater. Chem. Phys. 59 (1999) 1-5
13. G. S. V. R. K. Choudary, P. Prameela, M. Chaitanya Varma, A. Mahesh Kumar and K. H. Rao, Indian Journal of Materials Science 2013 (2013) 7 pages
14. S. M. Kabbur, U. R. Ghodake, D. Y. Nadargi, Rahul C. Kambale and S. S. Suryavanshi, J. Magn. Magn. Mater. 451(2018)665-675
15. A. Mahesh Kumar, M. Chaitanya Varma, G. S. V. R. K. Choudary, K. Srinivasa Rao, K. H. Rao and G. Gopalakrishna, Journal of Optoelectronics and Advanced Materials 12(2010)2386-2390
16. J. H. Nam, H. H. Jung, J. Y. Shin, and J. H. Oh, IEEE TRANSACTIONS ON MAGNETICS, 31(1995)3985-3987

17. J. J Shrotri, S. D. Kulkarni , C. E. Deshpande, Mater. Chem. Phys.59(1999)1-5.
18. Jun Xiang, XiangqianShen ,FuzhanSong, MingquanLiu , J.Solid State Chem.183 (2010) 1239–1244.
19. K.Srinivasa Rao, P.Appa Rao, M. Chaitanya Varma and K.H.Rao, J. Alloys Compd. 750(2018)838-847
20. B. Parvatheswar Rao and KHRao, J. Mater. Sci. Lett. 22 (2003) 1607
21. S. Zahi, A. R. Daud, M. Hashim, Mater. Chem. Phys.106 (2007) 452-456.
22. J.J. Shrotri, S.D. Kulkarni, C.E. Deshpande, A. Mitra, S.R. Sainkar, P.S. Anil Kumar and S.K. Date, Mater. Chem. Phys. 59 (1999) 1-5
23. Z.H.Khan, M.Mahbubur Rahman, S.S.Sikder, M.A.Hakim and D.K.Saha, J. Alloys Compd. 548(2013)208-215

